

The Design of Optical Signal Transforms Based on Planar Waveguides on a Silicon on Insulator Platform

Trung-Thanh Le

Abstract— This paper proposes new designs for optical signal processing elements based on solely on the combination of single mode waveguides and 2x2 multimode interference (MMI) couplers on a silicon-on-insulator (SOI) platform. For the first time, it is shown how optical Hadamard and Haar wavelet transforms may be implemented on an SOI platform using these passive planar devices. The designs for these devices are optimized using the three dimensional beam propagation method (3D BPM).

Index Terms— Optical waveguides, multimode interference devices, optical signal processing, optical transforms.

I. INTRODUCTION

For many years, optical techniques have been considered for a variety of signal processing tasks such as pattern recognition, the generation of ambiguity surfaces for radar signal processing and image processing applications [1]. Early efforts used lens systems, fibre-optics or directional couplers to develop optical signal processing transformers such as the Hadamard transform, and the discrete Fourier transform (DFT). Recently, there has been renewed research interest in optical signal processing transformers for quantum cryptography and other telecommunication applications.

Over the past decade or so there has been also much interest in using multimode interference (MMI) devices in optical coupling and switching applications, due to their advantages of low loss, compactness and good fabrication tolerances. These properties allow MMI based devices to be integrated with other devices on a photonic chip. The available material systems used for such photonic circuits include polymers, silica on silicon and silicon-on-insulator (SOI). The high-index contrast silicon-on-insulator (SOI) platform has attracted much interest due to its potential for miniaturization, improved performance, and compatibility with existing CMOS technology [3], [4].

It transpires that the MMI coupler is also a useful element in optical signal processing since the basic operations of sum and difference, and exchange, can be performed simply using MMI structures with some small modifications. Therefore,

Manuscript received October 16, 2009

Trung-Thanh Le was with Department of Electronic Engineering, La Trobe University, Australia. (Phone: +61-3-9479 3731; e-mail: thanh.latrobe@gmail.com). He is now with the Department of Information Technology, The College of Natural Resources and Environment, Hanoi, Vietnam.

various signal processing devices can be implemented using multimode interference structures [5], [6].

The objective of this paper is to propose methods for designing building blocks for photonic signal processing circuits using only passive MMI structures and single mode waveguides. These devices are designed and optimized with the 3D BPM method. Finally, optimized designs for optical discrete Hadamard and Haar transforms based on the SOI platform are presented.

II. DESIGNS OF BUILDING BLOCKS FOR OPTICAL SIGNAL PROCESSING

A. Synthesis of basic elements using 2x2 MMI couplers and phase shifters

The low pass and high pass filters associated with the Hadamard, Haar wavelet filter (H_1) or the Daubechies wavelet filter of order M=1 can be written as [7]

$$H_1 = \begin{bmatrix} H \\ G \end{bmatrix} = \frac{1}{\sqrt{2}} \begin{bmatrix} 1 & 1 \\ 1 & -1 \end{bmatrix} \quad (1)$$

The above transfer matrix provides the sum and difference operations that are the core of many signal processing functions.

It is interesting to note that the transfer matrix describing the relation between the input and output fields of a 2x2 restricted interference ideal MMI coupler (RI MMI) of length $L_\pi/2$ is [8]

$$\mathbf{M}_{RI} = \frac{e^{j\phi_{RI}}}{\sqrt{2}} \begin{bmatrix} 1 & j \\ j & 1 \end{bmatrix} \quad (2)$$

where ϕ_{RI} is a constant phase, $L_\pi = \frac{\pi}{\beta_0 - \beta_1}$ is the beat length of the two lowest order modes of the coupler having propagation constants of β_0 and β_1 , respectively.

Similarly, the transfer matrix for an ideal 2x2 general interference MMI (GI MMI) coupler of length $3L_\pi/2$ can be written as

$$\mathbf{M}_{GI} = \frac{e^{j\phi_{GI}}}{\sqrt{2}} \begin{bmatrix} 1 & -j \\ -j & 1 \end{bmatrix} \quad (3)$$

where ϕ_{GI} is a constant phase of the GI MMI coupler. By

adding phase shifters at the input and output waveguides for a 2x2 RI MMI coupler and a 2x2 GI MMI coupler as shown in Fig. 1(a), (b), (c), and (d) respectively, the overall transfer function for both couplers has the form

$$\mathbf{M}_\phi = \frac{e^{j\phi}}{\sqrt{2}} \begin{bmatrix} 1 & 1 \\ 1 & -1 \end{bmatrix} \quad (4)$$

where $\phi = \phi_{RI}$ or $\phi = \phi_{GI}$ depending on the RI or GI MMI coupler used.

We can see that (4) has the same general form as the first order Haar transform without the phase factor. For simplicity, this phase factor is neglected in the following analyses and designs.

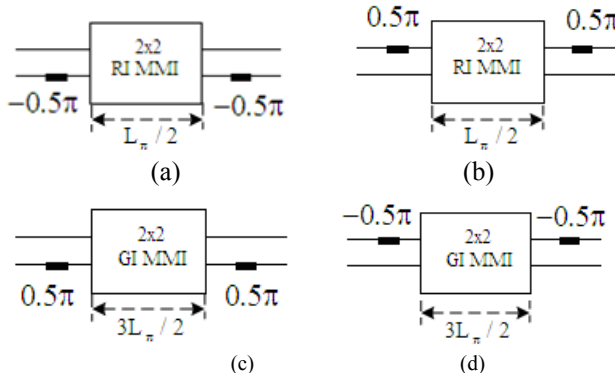


Fig. 1 The first order (2-point) Haar wavelet filter is realized by the use of (a), (b) 2x2 RI and (c), (d) GI-MMI couplers

Next, an exchange unit can be formed from an ideal 2x2 RI-MMI coupler of length L_π , which has a transfer matrix S_{RI} given by

$$S_{RI} = je^{j2\phi_{RI}} \begin{bmatrix} 0 & 1 \\ 1 & 0 \end{bmatrix} = e^{j(2\phi_{RI} + \frac{\pi}{2})} \begin{bmatrix} 0 & 1 \\ 1 & 0 \end{bmatrix} \quad (5)$$

Note that there will be a phase shift of $2\phi_{RI} + \frac{\pi}{2}$

introduced to both outputs. The exchange unit and its circuit symbol are shown in Fig. 2(a) and 2(b), respectively.

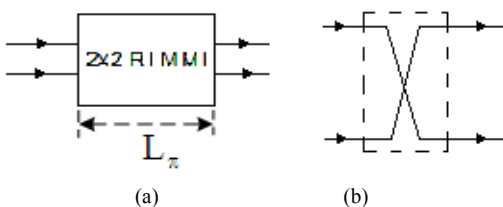


Fig. 2 (a) Exchange unit (a) using a 2x2 RI-MMI coupler and (b) its circuit symbol

Similarly, the transfer matrix for a 2x2 GI MMI coupler of length $3L_\pi$ is given by

$$S_{GI2} = -je^{j2\phi_{GI}} \begin{bmatrix} 0 & 1 \\ 1 & 0 \end{bmatrix} = e^{j(2\phi_{GI} - \frac{\pi}{2})} \begin{bmatrix} 0 & 1 \\ 1 & 0 \end{bmatrix} \quad (6)$$

Therefore, the exchange unit can be implemented by using a 2x2 GI MMI coupler with additional phase shifts added to the output waveguides as shown in Fig. 3.

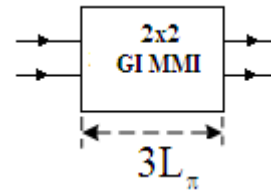


Fig. 3 Exchange unit realized with a 2x2 GI MMI coupler of length $3L_\pi$

Another way to realize the first order Haar transform is to use a Mach Zehnder interferometer (MZI) structure, which comprises two 3dB MMI couplers connected to each other with a phase shift $\Delta\phi$ between them as shown in Fig. 4.



Fig. 4 Realization of the first order Haar transform by using a MZI structure

In this case, the overall transfer matrix is given by:

(a) For a 3dB RI MMI coupler

$$S = je^{j2\phi_{RI}} e^{j\frac{\Delta\phi}{2}} \begin{bmatrix} \sin \frac{\Delta\phi}{2} & \cos \frac{\Delta\phi}{2} \\ \cos \frac{\Delta\phi}{2} & -\sin \frac{\Delta\phi}{2} \end{bmatrix} \quad (7)$$

and (b) for a 3dB GI MMI coupler

$$S = je^{j2\phi_{GI}} e^{j\frac{\Delta\phi}{2}} \begin{bmatrix} \sin \frac{\Delta\phi}{2} & \cos \frac{\Delta\phi}{2} \\ \cos \frac{\Delta\phi}{2} & -\sin \frac{\Delta\phi}{2} \end{bmatrix} \quad (8)$$

Therefore, the first order Haar transform can be obtained by the use of this structure if the phase shift $\Delta\phi = \frac{\pi}{2}$.

In the next section, we discuss the synthesis method of Hadamard transforms and discrete Haar transforms by using the above basic signal processing elements.

B. Synthesis of Hadamard transform

The synthesis of Hadamard transforms using MMI structures has been proposed previously by Gupta et al. [5]. However, the 4x4 Hadamard transform was not implemented in that paper. Also, all the Hadamard transforms given by Gupta et al. are synthesized by using RI MMI couplers. Here, a synthesis method for the 4x4 Hadamard transform using both GI and RI MMI couplers is presented.

The 4x4 Hadamard transform is described by a 4x4 Hadamard matrix given by

$$HD_4 = \begin{bmatrix} 1 & 1 & 1 & 1 \\ 1 & 1 & -1 & -1 \\ 1 & -1 & 1 & -1 \\ 1 & -1 & -1 & 1 \end{bmatrix} \quad (10)$$

In order to use the above basic operation units, this matrix could be factorized by the following relation

$$HD_4 = \begin{bmatrix} 1 & 1 & 0 & 0 \\ 1 & -1 & 0 & 0 \\ 0 & 0 & 1 & 1 \\ 0 & 0 & 1 & -1 \end{bmatrix} \begin{bmatrix} 1 & 0 & 0 & 0 \\ 0 & 0 & 1 & 0 \\ 0 & 1 & 0 & 0 \\ 0 & 0 & 0 & 1 \end{bmatrix} \quad (11)$$

$$\begin{bmatrix} 1 & 1 & 0 & 0 \\ 1 & -1 & 0 & 0 \\ 0 & 0 & 1 & 1 \\ 0 & 0 & 1 & -1 \end{bmatrix} \begin{bmatrix} 1 & 0 & 0 & 0 \\ 0 & 0 & 1 & 0 \\ 0 & 1 & 0 & 0 \\ 0 & 0 & 0 & 1 \end{bmatrix}$$

Then the 4×4 Hadamard transformer can be realized by cascading four stages as shown in Fig. 5(a). This structure requires four first order Hadamard transforms and two exchange units.

In a practical design, the number of the phase shifters should be minimized. After rearranging the phase shifters and choosing the proper designs for the exchange operation units and the Haar transform, the circuit for the Hadamard transform can be implemented as illustrated in Fig. 5(b). This structure requires a minimum number of phase shifters. In practice, the phase shifts may be obtained by using tapered sections or by using pattern relief techniques on the SOI waveguides as described in the earlier section. Note that the phase shift over the length of the outer optical waveguides needs to be the same as the phase shift through the exchange unit. This ensures that the signals arrive at the next stage with the correct relative phases. Thus, we need to add a compensating phase shift ϕ_D to the outer waveguides

$$\phi_D = \frac{2\pi}{\lambda_0} n_{eff} L_{MMI} - \arg(r_{GI}) \quad (12)$$

where n_{eff} is the refractive index of the TE fundamental mode of the optical waveguide, L_{MMI} is the length of the exchange unit formed by using the 2×2 GI MMI coupler, and $\arg(r_{GI})$ is the phase associated with the phase factor r_{GI} in (3). Also, we need to add additional (relative) phase shifts to the outer waveguides to provide the correct phase shifts for the sum and difference units and the exchange units (also see Fig. 1 and Fig. 3).

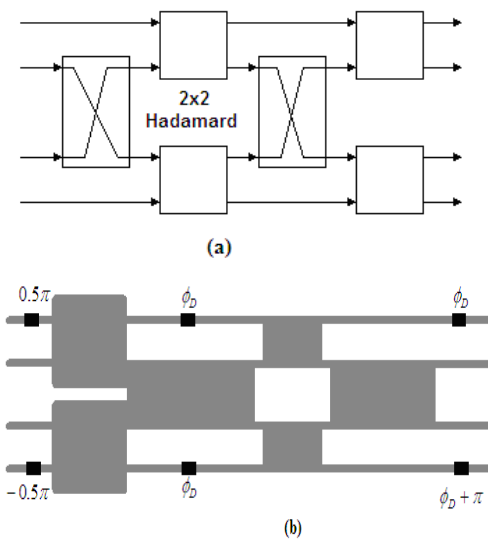


Fig. 5 Synthesis of a 4×4 Hadamard transformer using 2×2 Haar transformers and exchange gates, (a) symbolic representation, and (b) circuit fabrication structure. The darker regions show the phase shifts

C. Synthesis of Haar transform

The Haar transform is useful in applications where real time implementation of edge detection or contour extraction is required [9]. We now propose a synthesis method for the realization of Haar transforms. This method is suitable for pipeline implementation.

The Haar transform is based on the Haar function which is periodic, orthogonal and complete. The first order Haar matrix is defined as

$$H_1 = \frac{1}{\sqrt{2}} \begin{bmatrix} 1 & 1 \\ 1 & -1 \end{bmatrix} \quad (13)$$

This device can be implemented by using the MMI couplers as mentioned above. For simplicity, the normalization constant factor $1/\sqrt{2}$ is omitted in the following designs.

The k^{th} order Haar matrix can be written as

$$H_k = \begin{bmatrix} H_{2^{k-1}} \otimes (1 \ 1) \\ I_{2^{k-1}} \otimes (1 \ -1) \end{bmatrix} \quad (14)$$

where \otimes is the Kronecker product and $I_{2^{k-1}}$ is an identity matrix of dimension 2^{k-1} . $H_0 = 1$.

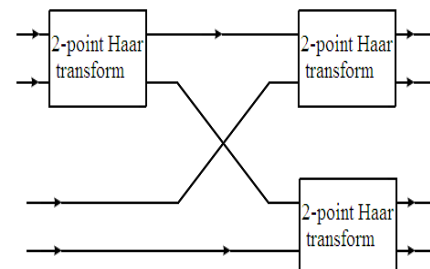
As an example, the second Haar matrix is given below

$$H_2 = \begin{bmatrix} 1 & 1 & 1 & 0 \\ 1 & 1 & -1 & 0 \\ 1 & -1 & 0 & 1 \\ 1 & -1 & 0 & -1 \end{bmatrix} \quad (15)$$

This matrix can be rewritten as

$$H_2 = \begin{bmatrix} 1 & 1 & 0 & 0 & 1 & 0 & 0 & 0 \\ 1 & -1 & 0 & 0 & 0 & 0 & 1 & 0 \\ 0 & 0 & 1 & 1 & 0 & 1 & 0 & 0 \\ 0 & 0 & 1 & -1 & 0 & 0 & 0 & 1 \end{bmatrix} \begin{bmatrix} 1 & 0 & 0 & 0 & 1 & 1 & 0 & 0 \\ 0 & 0 & 1 & 0 & 1 & -1 & 0 & 0 \\ 0 & 1 & 0 & 0 & 0 & 0 & 1 & 1 \\ 0 & 0 & 0 & 1 & 0 & 0 & 0 & -1 \end{bmatrix} \quad (16)$$

As a result, the 4-point Haar as shown in Fig. 6(a) or in Fig. 6(b). In Fig. 6(a), the structure requires transform can be realized by cascading three stages of 2-point Haar transform three 2-point Haar transforms and an exchange unit. Alternatively, the structure in Fig. 6(b) needs curved waveguides to guide the output data, so the former structure is preferred when the device is designed for the optical domain.



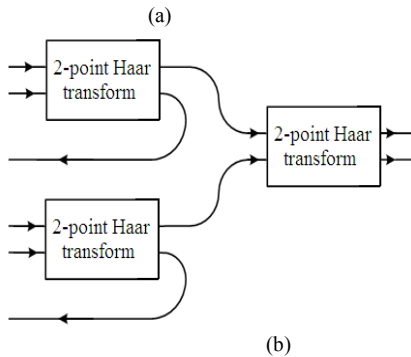


Fig. 6 4-point Haar transform using 2-point Haar transforms and exchange units (a) the structure for computing the 4-point Haar transform and (b) an equivalent structure

For example, the 4-point Haar transform can be realized by cascading 2×2 GI-MMI structures and phase shifters as shown in Fig. 6(a). In this design, 2×2 GI-MMI structures are used because it is easier to cascade these devices due to their large separation between access waveguides. For obvious practical reasons, the number of phase shifters in the structure of Fig. 7 has been minimized. Note that the phase shift over the length of the outer optical waveguides needs to be the same as the phase shift through the first 2-point Haar transform unit. This ensures that the signals arrive at the next stage with the correct relative phases. For this reason, a compensating phase shift ϕ_{D1} needs to be added to the outer waveguides.

$$\phi_{D1} = \frac{2\pi}{\lambda} n_e L_{MMI} - \phi_{GI} \quad (17)$$

where n_e is the refractive index of the fundamental TE mode of the optical waveguide, L_{MMI} is the length of the exchange unit formed by using the 2×2 GI-MMI coupler, and ϕ_{GI} is the phase associated with the GI-MMI coupler. In practice, ϕ_{GI} also includes any additional phase shift due to the tapered waveguides at the input and output ports of MMI couplers. Also, additional (relative) phase shifts need to be added to the outer waveguides to provide the correct phase shift ϕ_{D2} for the exchange unit having a length of $3L_\pi$.

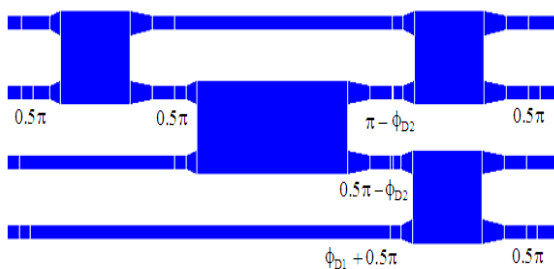


Fig. 7 A photonic circuit for implementing the 4-point Haar transform using the GI-MMI structures

The higher order Haar transforms ($N \times N$ or N -point Haar transform) can also be implemented in terms of lower order Haar transforms. For example, the 8-point Haar transform can be implemented by a suitable connection of 2-point Haar transforms as shown symbolically in Fig. 8.

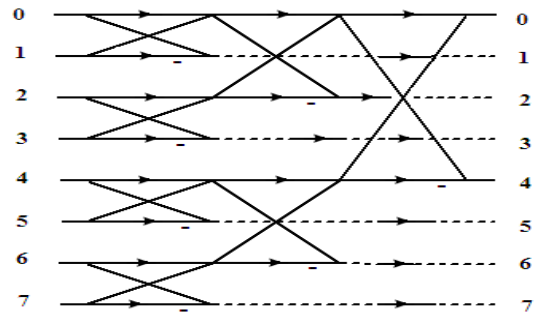


Fig. 8 Symbolic representation (signal flow graph) of the 8-point Haar transform

The pipeline architecture of the 8×8 Haar transform can be implemented as shown in Fig. 9. A total of $(N-1)$ 2-point Haar transforms are required in this case.

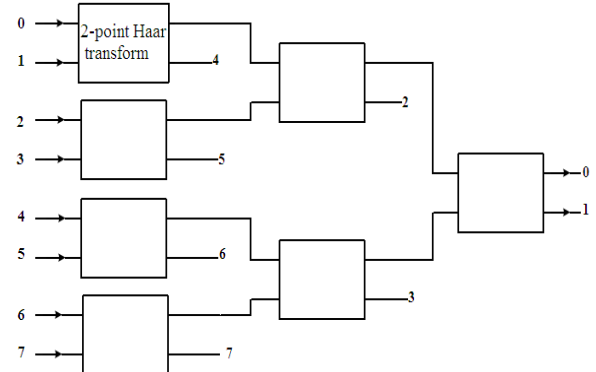


Fig. 9 Synthesis of the 8-point Haar transform using the 2-point Haar transforms

III. SIMULATION RESULTS AND DISCUSSIONS

In this section, the above devices are designed on an SOI platform. The waveguide structure is shown in Fig. 10. The parameters used in our simulations are as follows: refractive index of silicon channel region $n_{Si} = 3.455$, the refractive index of the silicon oxide region $n_{SiO_2} = 1.46$, the width of the MMI $W_{MMI} = 6\mu m$, the Si thickness $h_{co} = 220nm$ and the access waveguide widths $W_{access} = 0.5 \mu m$. Tapered waveguides having a length of $5\mu m$ are used for connecting the access waveguides to the MMI sections in order to improve the device performance. The wavelength is $\lambda = 1550nm$. All the simulations are based on TE mode propagation.

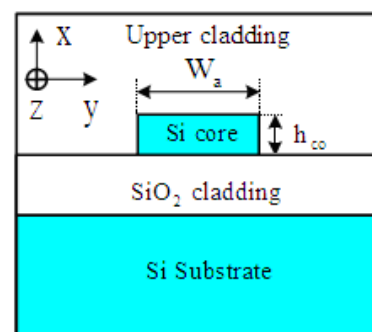


Fig. 10 Waveguide structure used in the simulations

Optimised design of the 2-point Haar transform: The 2-point Haar transform unit can be implemented by using both 2x2 GI and RI-MMI couplers with the aid of the phase shifters. The aim here is to optimise these devices on the SOI platform. The first step is to optimise the MMI sections. The multimode sections need to be wide enough to achieve good performance and to be spaced apart sufficiently to limit crosstalk between the adjacent access waveguides. It is assumed that the width of the MMI waveguide is 4 μm for the 2-point Haar transform based on the RI theory and is 3 μm for the 2-point Haar transform based on the GI theory.

First, the wide-angle 3D-BPM is used to carry out the simulations for the device having a length of 30 μm for the 2x2 RI-MMI coupler and a length of 40 μm for the 2x2 GI-MMI coupler. The aim of this step is to find roughly the positions which result in a power splitting of 50/50, i.e., a 3dB coupler. Then, the 3D-BPM is used to perform the simulations around these positions to locate the best lengths. The transmission of the 2x2 RI-MMI coupler at different lengths of the couplers are plotted in Fig. 11. The simulations show that the optimised length for obtaining the best performance with the chosen parameters is 20 μm .

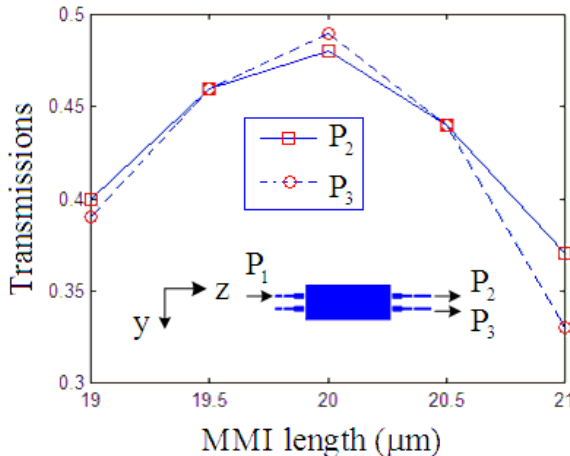


Fig. 11 The normalized output powers at the bar and cross ports at different lengths of a 2x2 RI-MMI coupler

The transmission of the 2x2 GI-MMI coupler at different lengths of the couplers are plotted in Fig. 12. The optimised length of the GI-MMI coupler is 34 μm .

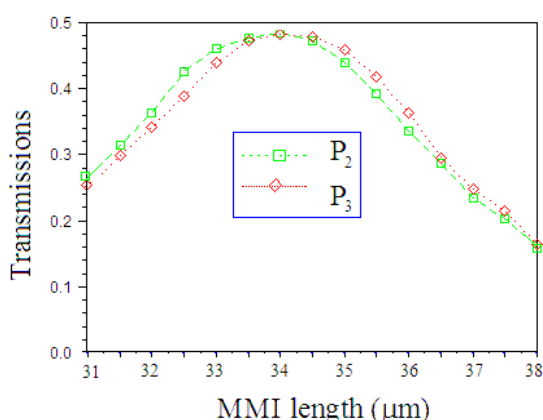


Fig. 12 The normalized output powers at the bar and cross ports with different lengths of a 2x2 GI-MMI coupler

The next step is to add the phase shifter to the previously optimised MMI sections. Note that the 2-point Haar transform requires the addition of a phase shift of $-\pi/2$ in the RI case and a phase shift of $\pi/2$ in the GI case to the bottom waveguides in the 2x2 3dB MMI couplers. Here, as an example, the phase shift is implemented by using the pattern technique as proposed in [10]. Patterns having widths of $W_p = 480\text{nm}$ and depths of $h_p = 40\text{nm}$ are used to make the desired phase shifts. From our calculations, the pattern length is $L_p = 2.5 \mu\text{m}$ to make a phase shift of $-\pi/2$.

The 3D-BPM simulations for optimised designs of the 2-point Haar transform using the 2x2 RI-MMI coupler and using the 2x2 GI-MMI coupler are shown in Fig. 13(a) and in Fig. 13(b), respectively. It is assumed that the two light beams at input ports 1 and 2 have the same phase and amplitude. The BPM simulations show that power only exits output port 1. The normalized output power is 0.96 and the excess loss is 0.18dB for both cases (RI-MMI and GI-MMI).

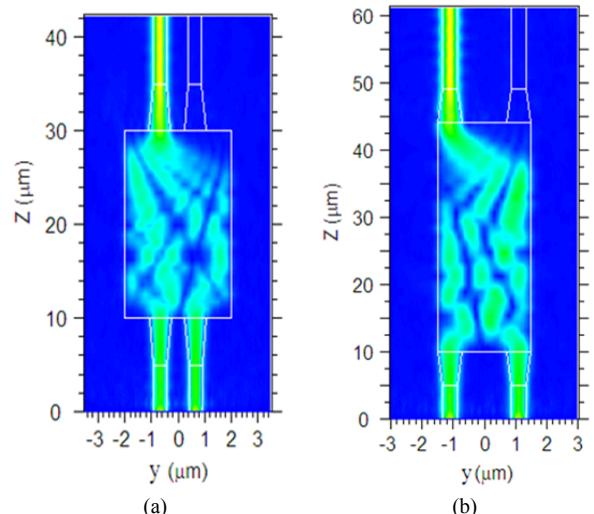


Fig. 13 The 3D-BPM simulation for the operation of the 2-point Haar transform (a) the transform using the 2x2 RI-MMI and (b) the transform using the 2x2 GI-MMI coupler

Optimised design of the exchange unit: The exchange unit can be realized using MMI couplers having the appropriate dimensions ($L_{\text{MMI}} = 3L_\pi / 2$ for 2x2 GI-MMI couplers and $L_{\text{MMI}} = L_\pi / 2$ for 2x2 RI-MMI couplers) to form a mirror image. Both RI and GI-MMI couplers can be employed to realize the exchange unit. The optimised lengths of the MMI coupler used for the exchange unit are 40 μm for the RI-MMI coupler and 67.3 μm for GI-MMI coupler. The calculated excess losses in both cases are 0.4dB.

The 3D-BPM simulations for the exchange unit having normalized powers of 0.8 and 0.2 presented at input ports 1 and 2 are plotted in Fig. 14(a) and 14(b), respectively.

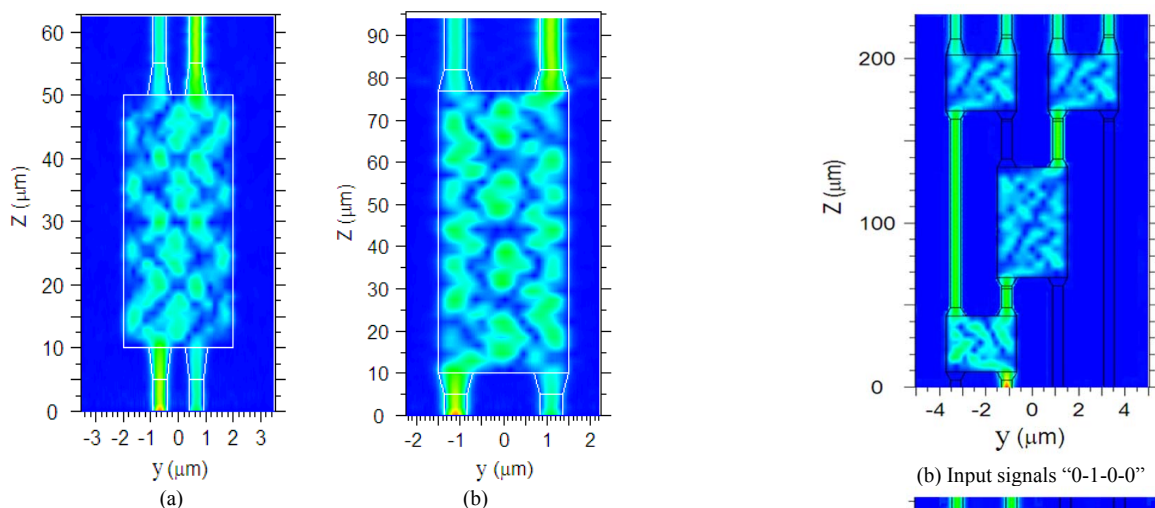
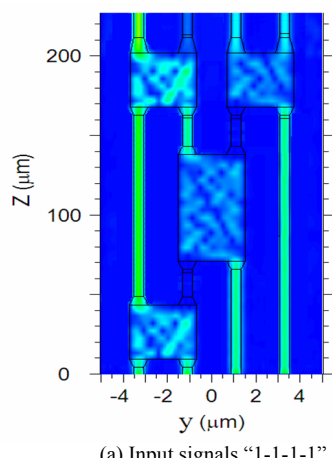


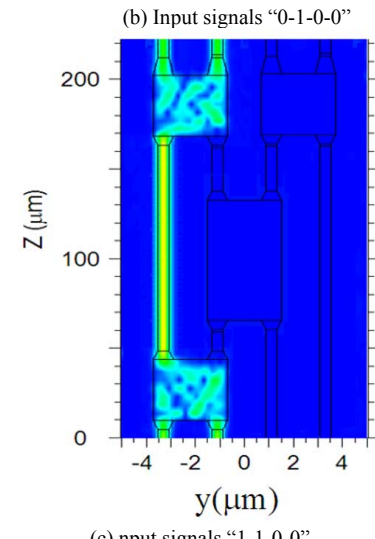
Fig. 14 The 3D-BPM simulations for an exchange unit based on (a) the RI-MMI theory and (b) the GI-MMI theory. The exchange is performed for two input signals having normalized powers of 0.8 and 0.2 at two input ports

Optimised design of the 4-point Haar transform: As an example, the 3D-BPM simulations of the 4-point Haar transform for three cases now will be presented. The first case is for input light beams applied to all input ports, simultaneously. The 3D-BPM simulation for this case is plotted in Fig. 15(a). The second case is for an input signal presented at input port 2 and the third case is for input signals presented at input ports 1 and 2. The simulations for these cases are displayed in Fig. 15(b) and 15(c). The simulations show that the device performs the functions of the 4-point Haar transform as predicted by the theory. The excess loss of this device is 0.95dB for the first case, 0.78dB for the second case and 0.48dB for the third case.

It is noted that the normalization factor $1/\sqrt{2}$ for high order Haar transforms in the theoretical analyses was neglected. In practice, it is necessary to add optical attenuators or optical amplifiers to the appropriate points in the circuit for realizing Haar transforms.



(a) Input signals “1-1-1-1”



(b) Input signals “0-1-0-0”

Fig. 15 The 3D-BPM simulations for the 4-point Haar transform with different input signals (a) input signals “1-1-1-1” presented at four input ports, (b) input signals “0-1-0-0” and (c) input signals “1-1-0-0”

IV. CONCLUSION

In this paper, we have presented a new method for the design of passive optical elements including optical signal transforms suitable for photonic signal processing applications. These elements can be comprised solely of MMI structures and single mode waveguides. The design of these devices for an SOI platform can be carried out in a straight-forward manner with the help of 3D BPM and mode solver software. Novel designs have been presented for implementation of the optical discrete Hadamard and Haar transforms. 3D-BPM simulations have shown that good performance can be obtained and that the devices may be cascaded to achieve more complex optical transforms. Such structures are particularly suitable for pipeline operation with low latency.

REFERENCES

- [1] M. Shirakawa, T. Takemori, and J. Ohtsubo, "Optical computing based on a selector logic," *Optics Communications*, vol. 124, No. 3-4, pp. 333-344, 1996
- [2] S. Tseng, Y. Kim, C. J. K. Richardson, and J. Goldhar, "Implementation of discrete unitary transformations by multimode waveguide holograms," *Applied Optics*, vol. 45, No. 20, pp. 4864-4872 2006.
- [3] I. P. Kaminow, T. Li, and A. Willner, *Optical Fiber Telecommunications V (A&B)*, vol. V: Elsevier, Academic Press, 2008.

- [4] I. P. Kaminow, "Optical Integrated Circuits: A Personal Perspective," *IEEE Journal of Lightwave Technology*, vol. 26, No. 9, pp. 994-1004, May 2008.
- [5] A. R. Gupta, K. Tsutsumi, and J. Nakayama, "Synthesis of Hadamard Transformers by Use of Multimode Interference Optical Waveguides," *Applied Optics*, vol. 42, pp. 2730-2738, 2003.
- [6] L. W. Cahill and T. T. Le, "Photonic Signal Processing using MMI Elements," presented at 10th International Conference on Transparent Optical Networks (ICTON 2008), Athens, Greece, 2008 (invited paper).
- [7] G. Cincotti, "Fiber wavelet filters," *IEEE Journal of Quantum Electronics*, vol. 38, No. 10, pp. 1420-1427, 2002.
- [8] M. Bachmann, P. A. Besse, and H. Melchior, "Overlapping-image multimode interference couplers with a reduced number of self-images for uniform and nonuniform power splitting," *Applied Optics*, vol. 34, pp. 6898-6910, 1995.
- [9] S. Burrus, R. A. Gopinath, and H. Guo, *Introduction to Wavelets and Wavelet Transforms: A Primer*: Prentice Hall, United States, 1997.
- [10] T. T. Le and L. W. Cahill, "The Design of Multimode Interference Couplers with Arbitrary Power Splitting Ratios on an SOI Platform," LEOS 2008, Newport Beach, California, USA, 9-14 Nov 2008.

Trung-Thanh Le received the B.Sc. and M.Sc. degrees in electronic and telecommunication engineering from Hanoi University of Technology, Vietnam in 2003 and 2005, respectively. He received the PhD degree in electronic engineering from La Trobe University, Australia in 2009. He has also been a lecturer at the College of Natural Resources and Environment, Hanoi, Vietnam.